Persistent Continental Shelf Carbon Sink at the Ieodo Ocean Research Station in the Northern East China Sea

Kitack Lee[1], Ja-Myung Kim[1]*, Gyeong-Seok Lee[1], Eunil Lee[2], Jin-Yong Jeong[3], Jaeik Lee[3] and In-Seong Han[4]

[1] Division of Environmental Science and Engineering, Pohang University of Science and Technology, Pohang, South Korea, [2] Ocean Research Division, Korea Hydrographic and Oceanographic Agency, Busan, South Korea, [3] Marine Domain Management Research Division, Korea Institute of Ocean Science and Technology, Busan, South Korea, [4] Ocean Climate and Ecology Research Division, National Institute of Fisheries Science, Busan, South Korea

Hourly (2017–2021) to seasonal (2015–2021) inorganic C data were collected at the Ieodo Ocean Research Station (32.07°N and 125.10°E) in the northern East China Sea (ECS), located under the influence of the nutrient-rich Changjiang Diluted Water (CDW). An increase in phytoplankton biomass from April to mid-August (the warming period) equalized much of the temperature-driven increase in the surface pCO_2 and thus, made the northern ECS a moderate sink of atmospheric CO_2. From November to March (the cooling period), a large pCO_2 reduction, driven by a temperature reduction, and a high air–sea CO_2 exchange rate, because of high windspeeds, transformed the basin into a substantial CO_2 sink, yielding an annual net C uptake of 61.7 g C m^{-2} yr^{-1}. The effects of biological production and temperature change on seawater pCO_2 (and thus, the net air–sea CO_2 flux) were decoupled each season and acted in concert to increase the net annual CO_2 sink by the region. The present study provided the observational and mechanistic lines of evidence for confirming "continental shelf C pump"—a mechanism in the shallow waters of the continental shelves that accumulate a significant amount of C (*via* reinforced cooling and promoted biological C uptake) that is transported from the basin surface waters to the interior of the adjacent deep ocean. In the future, an increasing input of anthropogenic nutrients into the northern ECS is likely to make the region a stronger CO_2 sink.

Keywords: East China Sea, Ieodo Ocean Research Station, net air–sea CO_2 flux, continental shelf C pump, anthropogenic nitrogen deposition, riverine nitrate, Changjiang Diluted Water

INTRODUCTION

Unlike major ocean basins, the role of coastal and marginal seas as an anthropogenic CO_2 reservoir has been studied less because the small surface area of the global marginal seas (only 7% of the world's ocean area) may only store small amounts of anthropogenic CO_2. Contrary to this paradigm, the marginal seas can absorb substantial amounts of anthropogenic CO_2 because the primary producers in

those locations use high nutrient loads from adjacent continents and hence, accelerate CO_2 transfer by substantially reducing the concentration of surface C (Lee et al., 2011; Najjar et al., 2018). Moreover, the interaction between the resultant planktonic organic matter deposited onto the shallow sediments and the overlying seawater can generate alkalinity, facilitating the transfer of additional anthropogenic CO_2 (Thomas et al., 2009). Intrinsically, the air–sea CO_2 flux in the coastal and marginal seas is subject to large variabilities with time and location because the complex interactions between natural (e.g., tidal cycle, upwelling, wind-driven mixing, freshwater input, eutrophication, and biological activity) and anthropogenic (e.g., inputs of anthropogenic C and nutrients and ocean temperature increase) factors make estimating the air–sea CO_2 flux challenging and often unsuccessful (Park et al., 2006; Dai et al., 2013; Cao et al., 2019). A major hurdle in carrying out such estimates is our inability to capture all major variabilities in the air–sea CO_2 flux over the extensive periods covering all seasons.

No exception to this generalization is the East China Sea (ECS), which has an extensive continental shelf covering two-thirds of its area and is surrounded by populated countries (i.e., China, Korea, and Japan). The CO_2 emissions from these countries fall within the top tier; however, the successful execution of reforestation in these countries has led to a substantial C uptake by the terrestrial biosphere (Choi et al., 2002; Piao et al., 2009). The ECS is teeming with plankton as a result of nutrient input by the Changjiang River. The addition of these river-borne nutrients has divided the ECS into two distinct regions in terms of nutrient concentration: the northern ECS, which is characterized more by the nutrient input from the Changjiang River (anthropogenic influence), and the central and southern basins, which are more influenced by water exchange with the Kuroshio Current, which lacks nutrients (natural influence) (Zhang et al., 2021). Tropical cyclones are also common in the ECS in summer and fall. To determine if the entire ECS is a net sink or source of atmospheric CO_2, the determination of the amount of CO_2 that enters the northern ECS (i.e., the areas located between 28.5–33.0°N and 122.5–126.0°E) is critical because this area can be a large C sink as a result of the proliferation of phytoplankton.

Another factor equally acute in determining seawater pCO_2 (and thereby net air–sea CO_2 flux) in the northern ECS is the seasonal temperature change. The seasonal temperature extremes in the ECS and the adjacent Yellow Sea ranged from 10°–20°C (colors in **Figure 1**), which are likely the largest seasonal temperature swings in the world's oceans and arise from a seasonal switchover between a hot and humid North Pacific air mass governing the summertime temperature of the ECS (also the Yellow Sea) and a cold and dry Siberian air mass governing the winter temperature of the same basins (Chang, 2004). From a thermodynamics perspective, a pCO_2 change of up to 190 µatm can occur when transitioning from summer to winter.

This study reports the results of 5 years (2017–2021) of high-frequency (obtained at 1 h intervals) C data collected at a midpoint (the Ieodo Ocean Research Station, also known as
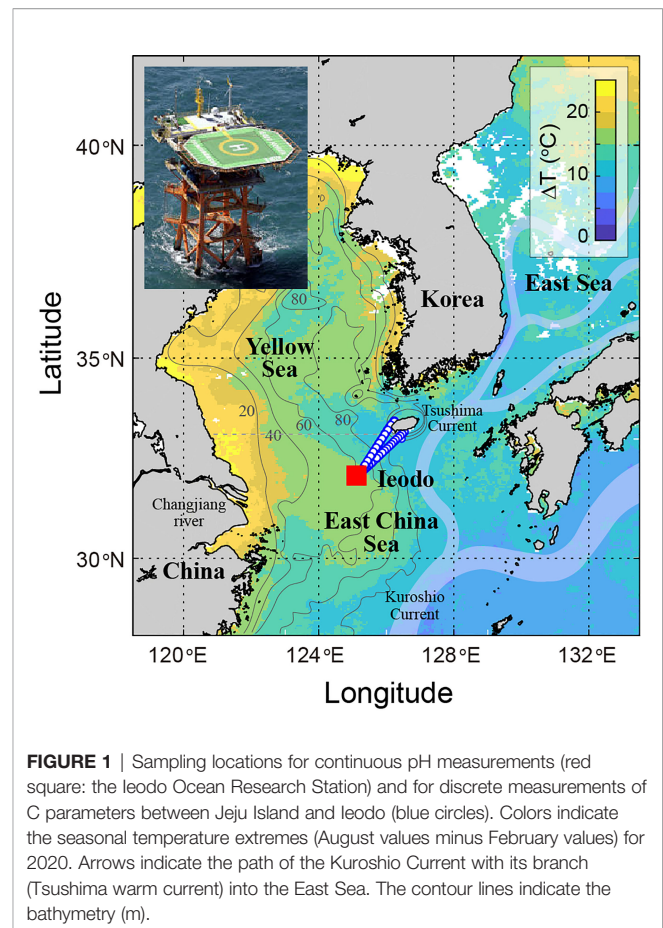

FIGURE 1 | Sampling locations for continuous pH measurements (red square: the Ieodo Ocean Research Station) and for discrete measurements of C parameters between Jeju Island and Ieodo (blue circles). Colors indicate the seasonal temperature extremes (August values minus February values) for 2020. Arrows indicate the path of the Kuroshio Current with its branch (Tsushima warm current) into the East Sea. The contour lines indicate the bathymetry (m).

Socotra Rock and Suyan Islet) between the mouth of the Changjiang River and Jeju Island, located downstream of the Changjiang freshwater plume in the northern ECS. The results of 7 years (2015–2021) of seasonal data obtained between Jeju Island and the Ieodo Ocean Research Station were added to substantiate the interpretation of the high frequency data. In parallel, we examined published data covering the northern ECS and concluded a basin-wide status of C sink. We also explored the key drivers of the C-sink status.

MATERIALS AND METHODS

Measurements of Total Alkalinity (A_T), Total Dissolved Inorganic Carbon (C_T), and pH

During the study period (2015-2021), at more than 50 locations between Jeju Island and the Ieodo Ocean Research Station (32.07°N and 125.10°E; halfway between the Changjiang River estuary, China and Jeju, Korea; hereafter referred to as "Ieodo"; **Figure 1**), we collected surface samples at seasonal intervals (April to December with no samples taken from January to March) for measurements of seawater C parameters. The measured C parameters were

total alkalinity (A_T = $[HCO_3^-]$ + $2[CO_3^{2-}]$ + $[B(OH)_4^-]$ + proton acceptors − $[H^+]$ − proton donors), total dissolved inorganic carbon (C_T = $[CO_2]$ + $[HCO_3^-]$ + $[CO_3^{2-}]$), and pH. The concentrations of A_T and C_T were determined using potentiometric and coulometric titrations, respectively. The precision of the A_T and C_T measurements were determined to be ± 1.8 µmol kg^{-1} for A_T and ± 2.2 µmol kg^{-1} for C_T (**Supplementary Figure 1**) by titrating reference materials with certified A_T and C_T values (provided by A. Dickson, Scripps Institution of Oceanography, USA). Small deviations of the measured A_T and C_T values on the reference materials from their certified values were either subtracted or added for sample measurements conducted during the same period in which the reference materials were analyzed. The pH was measured at 25°C spectrophotometrically using the m-cresol purple indicator following the procedure documented elsewhere (Clayton and Byrne, 1993; Lee et al., 1996).

Other CO_2 parameters (i.e., CO_2 partial pressure, pCO_2; seawater saturation state with respect to aragonite, Ω_{arag}) were calculated from the values of A_T and C_T using the set of the thermodynamic constants, including the carbonic acid dissociation constants reported by Mehrbach et al. (1973) and other ancillary constants proposed by Millero (1995). The thermodynamic model, including these dissociation constants, led to the best agreement between measurements and calculations involving all three measured parameters (A_T, C_T, and pH), as demonstrated in previous studies (McElligott et al., 1998; Lee et al., 2000; Lueker et al., 2000; Millero et al., 2006; Fong and Dickson, 2019). The agreement was compelling evidence for insignificant biases in A_T derived from organic acids (Cai et al., 1998; Kim and Lee, 2009; Ko et al., 2016) and phytoplankton and bacteria cells (Lee et al., 2021). The B:Cl ratio of 0.2414 confirmed for the open ocean (Lee et al., 2010) was shown to be accurate in the study area and in experiments designed to predict the borate contribution to A_T (Lee et al., 2019).

Continuous Seawater pH Measurements

Beginning in September 2017, seawater pH was measured at a depth of 4 m at 1 h intervals using a pH sensor package equipped with an ion-sensitive field effect transistor (ISFET), which produces stable pH signals; the sensor package also included a data logger based on a Honeywell Durafet pH sensor. The ISFET sensor was determined to be precise within ±0.005 pH units over periods of weeks to months. The pH sensor package (including temperature and salinity) was protected by a perforated copper guard, which deterred biofouling. The pH values were determined on the total scale at *in situ* temperature and salinity. During the period of deployment, we visited the site at seasonal intervals to check for signs of sensor drift. At each visit, we sampled seawater in close proximity (within the 10 m) of the sensor package 3 to 5 times per day over 2 days and analyzed their pH and salinity in the laboratory. A total of 70 samples were collected at Ieodo during a total of 8 visits over a 4 year period. A comparison between the sensor-based and laboratory-based pH measurements indicated that the sensor-based pH data showed no sign of drift over 6 months and were consistent with the laboratory measurements to within ±0.03 pH units

(**Supplementary Figure 2**). During each site visit, we downloaded the pH, salinity, and temperature data from the data logger, thoroughly cleaned the sensor package, and then redeployed it.

Polynomial Model for Predicting A_T

Empirical algorithms that relate A_T to sea surface salinity (S) and sea surface temperature (T) have been used to construct the distribution of A_T in regions (Lee et al., 2006) and have greatly facilitated predictions of the CO_2 flux across the air–sea interface, where it combines with another carbon parameter. A functional form for fitting A_T data was derived from datasets obtained within the 10 km of Ieodo (n = 162) by testing its polynomial form (first or second order) with two predictor variables (S and T) which gave a fit.

$$A_T = 2249.7 \\ + 2.48\,(S - 31.2) - 2.13\,(S - 31.2)^2 - 3.24\,(T - 21.8) \\ + 0.15\,(T - 21.8)^2$$

$$(1)$$

where 31.2 and 21.8 represent the mean values of S and T (°C) values, respectively. We found that the second-order polynomial model yielded the lowest value of the root-mean-square error (RMSE: the standard deviation of the predicted errors; 9.8), the highest value of r^2 (0.92), and the lowest value of p (< 0.05) (**Figure 2**). Because the A_T data (used to derive the fit) covered four seasons and seven years, the fit would represent seasonal and interannual variations in A_T.
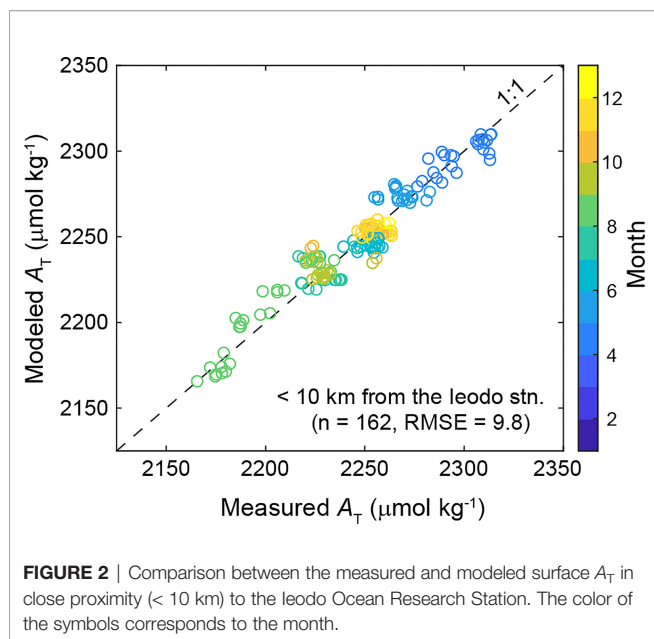
Air–Sea CO_2 flux

The air–sea CO_2 flux (mol C area^{-1} time^{-1}) across the air–water interface was calculated using the formula: $K_0 \cdot k(pCO_2^{air} - pCO_2^{sw})$. In this formula K_0 (mol L^{-1} atm^{-1}) is the CO_2 gas solubility, and k (cm hr^{-1}) is equal to $0.251\,U_{10}^2\,(Sc/660)^{-0.5}$, where U_{10} (m s^{-1}) is the windspeed at 10 m above sea level and Sc is the Schmidt number (Wanninkhof, 2014). Windspeed data measured at 33.08°N and 126.03°E, in the vicinity of the sampling site, are available at the National Climate Data Center. Air pCO_2^{air} data were obtained from the observatory at Anmyeondo (36.54°N, 126.33°E), which is operated by the Korea Meteorological Administration. Seawater pCO_2^{sw} data were calculated from pH measurements and A_T values derived from Equation (1), and thus had a probable error of < 30 µatm because of pH and A_T errors (±0.03 and ±10 µmol kg^{-1}, respectively). The resulting pCO_2^{sw} error was directly translated into a flux error of ±0.002 g C m^{-2} hr^{-1}.

RESULTS

Variations in Seawater C Parameters between Ieodo and Jeju Island

A notable feature found between Ieodo and Jeju Island in the northern ECS, located downstream of the Changjiang Diluted Water (CDW), is the large seasonal variability in salinity (26–35)

FIGURE 2 | Comparison between the measured and modeled surface A_T in close proximity (< 10 km) to the Ieodo Ocean Research Station. The color of the symbols corresponds to the month.

(**Figure 3A**). Much of the seasonal variability is directly associated with changes in the intrusion of the CDW sourced from the Changjiang Estuary. Specifically, the values of salinity at Ieodo decreased by as much as $S = 9$, which corresponds to the maximum intrusion of the CDW into the study area between July and August. The decrease in salinity also varied considerably interannually and was found to be the highest at Ieodo and to decrease toward Jeju Island. This salinity decrease was broadly proportional to the increase in intrusion of the CDW. The intrusion of the CDW into the study area was particularly pronounced in the summer of 2017, when the CDW propagated eastward and even reached the coastal waters near Jeju Island, close to southern Korea.

The intrusion of CDW into the northern ECS affected not only the salinity but also all of the C parameters, including *in situ* pCO_2 (175–490 µatm), pH (8.0–8.3), and Ω_{arag} (2.0–5.8) (**Figures 3D–F**). The gradients in four C parameters observed between Ieodo and Jeju Island were particularly pronounced during the summer months (June–August). The summertime pCO_2 values at Ieodo often remained less than 300 µatm, considerably lower than the current atmospheric pCO_2 of ~420 µatm and thus, the air–sea pCO_2 disequilibrium was highest at Ieodo and decreased toward Jeju Island (**Figure 3D**). The summertime pH distribution was opposite to that of pCO_2 because both parameters changed in opposite directions in response to changes in the same environmental factors (e.g., temperature, salinity, photosynthesis, and respiration) (**Figure 3E**). The highest Ω_{arag} values were observed at Ieodo and decreased toward Jeju Island (**Figure 3F**). One striking characteristic of the CDW was unusually high values of the salinity-normalized A_T (nA_T) and salinity-normalized C_T (nC_T) (**Figures 3B, C**), which were a direct consequence of high A_T and C_T values of the Changjiang River at salinity ≈ 0. The greater contribution of the Changjiang River led to the higher nA_T and

nC_T values of the CDW. Conversely, with increasing distance from the Changjiang Estuary, the values of nA_T and nC_T in the CDW rapidly decreased as a result of mixing with the warm current of Tsushima with low nA_T and nC_T values. In other months, the Ieodo–Jeju gradients in salinity and all of the CO_2 parameters either substantially decreased or disappeared completely.

Seawater pCO_2 and Net Air–Sea CO_2 Flux at Ieodo

The low levels of summertime pCO_2, between Ieodo and Jeju, were further substantiated by continuous pCO_2 measurements at Ieodo (**Figure 4C**). During the warming period (from April to mid-August), the surface pCO_2 values at Ieodo remained ~125 µatm lower than the atmospheric pCO_2. The magnitude of the air–sea disequilibrium differed slightly by year. However, the basin switched to a neutral condition in terms of the seawater pCO_2 level from September to October, with large temporal variability, which made the status of the basin as a net C sink or a net C source ambiguous. Moreover, the timing of the switchover from the lower-than-atmospheric pCO_2 condition to the higher-than-atmospheric pCO_2 condition differed by year. The switchover occurred in early September in 2019 (**Figure 5C**); however, it occurred late August in 2020, when the site was hit by Typhoon Bavi (**Figure 5D**).

Following this short transition period, the surface pCO_2 levels progressively decreased as the season transitioned to a full winter condition and were persistently 35–130 µatm lower than the atmospheric pCO_2 levels during the cooling period (November–March), with small temporal variations (**Figure 4C**). The measured decrease in surface pCO_2 from the late-summer condition to the full winter condition was approximately consistent with thermodynamic predictions based on the seasonal temperature decrease (**Figure 6B**). Both the under-saturated pCO_2 condition and high windspeeds led to a persistent C sink status of the basin (**Figure 4A, D**). Collectively, the year-round continuous data (2020–2021) show that the perennial C sink during both the warming (0.13 g C m^{-2} d^{-1}; from April to mid-August) and the majority of the cooling periods (0.32 g C m^{-2} d^{-1}; from November to March), along with a small source for a short transition period, led the region to a strong annual sink of atmospheric CO_2 (61.7 g C m^{-2} yr^{-1}).

Effects of Typhoons on Net Air–Sea CO_2 Flux at Ieodo

In the period 2019–2020, Ieodo was hit by seven major typhoons (four typhoons in 2019 and three in 2020). The ocean CO_2 system responded to those typhoons differently, depending on the timings of the typhoons' passage. The three typhoons that struck the site during the warming period accelerated ocean CO_2 uptake during their passages (see **Figures 5A, B**). The warming-period enhancement of ocean CO_2 uptake during the typhoon passage was an order of magnitude greater than those for periods either before or after the typhoon passage. The greater ocean CO_2 uptake during the typhoon passage was a consequence of the combined effects of sustained low pCO_2 levels and a high rate of CO_2 exchange. To our surprise, typhoons exerted the opposite
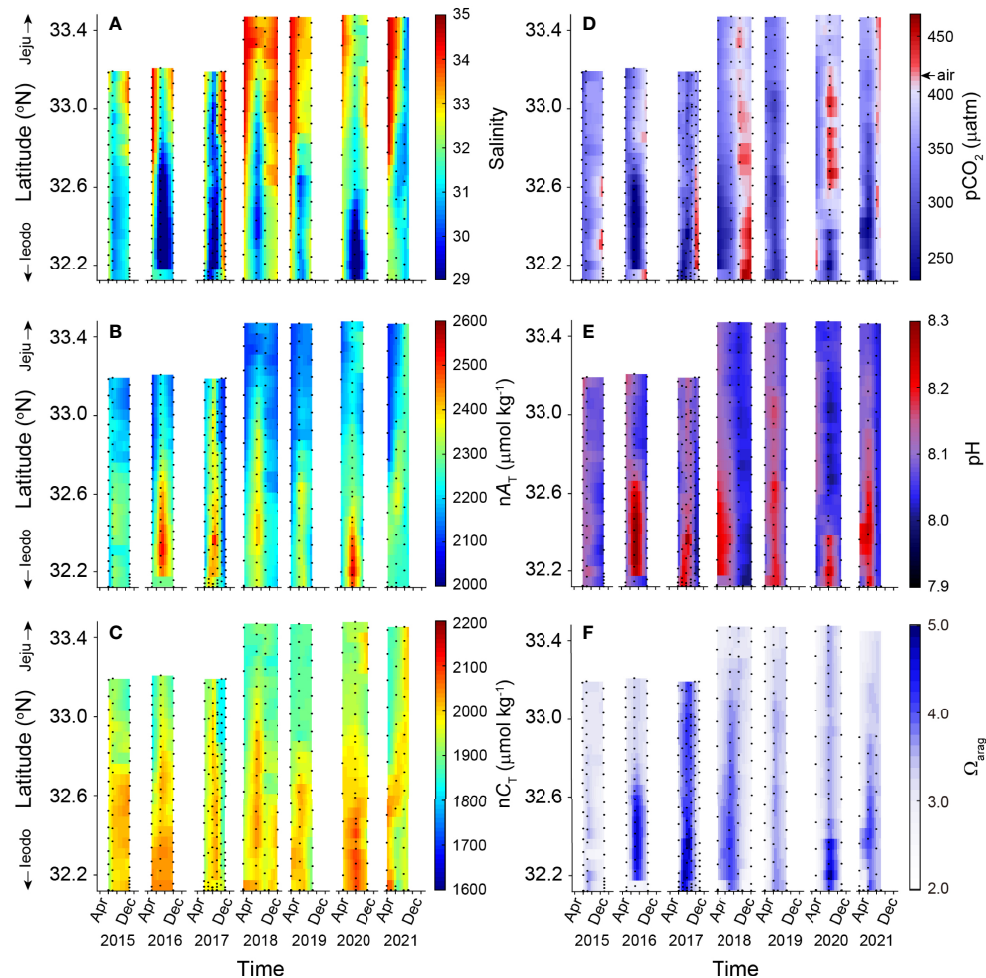
FIGURE 3 | Meridional distributions of **(A)** salinity, **(B)** salinity-normalized A_T (nA_T), **(C)** salinity-normalized C_T (nC_T), **(D)** seawater pCO$_2$, **(E)** pH, and **(F)** aragonite saturation state (Ω_{arag}). Longitudes covary along the survey line (125.17–126.55°E) between Ieodo and Jeju Island. The lower the latitude, the closer to Ieodo.

effect on the net air–sea CO$_2$ flux during the cooling period, when oceanic pCO$_2$ levels were higher than the atmospheric levels (**Figures 5C, D**). The typhoon-induced high surface pCO$_2$ levels resulted in unusually high effluxes (~7 times greater than the CO$_2$ fluxes that occurred during the typical cooling period).

DISCUSSION

Status of C Uptake by the ECS

In the ECS, the major controls of the seasonality in terms of the air–sea CO$_2$ flux differed regionally: the northern ECS was dominated by biological activities and ventilation of water, whereas the central and southern ECS were mainly determined by seawater temperature (Guo et al., 2015; Deng et al., 2021). With regard to the status of net air–sea CO$_2$ flux across the entire ECS, mixed conclusions have been reported in literature, in part because the datasets that led to differing conclusions did not cover time and space extensively (Deng et al., 2021 and

references therein). Specifically, the datasets were skewed to either the Chinese coastal waters under the direct influence of the nutrient-rich CDW (Li et al., 2021; Wu et al., 2021) or the offshore waters distant from the CDW influence (Shim et al., 2007; Kim et al., 2013). Overall, the entire ECS appeared to be a slight C sink on an annual scale (Wang et al., 2000; Zhai and Dai, 2009; Guo et al., 2015; Wu et al., 2021), although it can be a weak C source when seasonal dynamics of river input and physical mixing occasionally induce C release in summer and fall in the inner shelves of the ECS (the Changjiang freshwater plume).

In comparison with the previous estimates based on either the data in a specific month or an empirical model (Wang et al., 2000; Tseng et al., 2011; Guo et al., 2015), our year-round measurements (2020–2021) in the northern ECS yielded the annual net air–sea CO$_2$ flux of 61.7 g C m^{-2} yr^{-1} (= 14.1 mmol C m^{-2} d^{-1} from air to sea), which was 2-3 times higher than the values reported for the adjacent regions. The air–sea CO$_2$ influx in summer (4.7 mmol C m^{-2} d^{-1}) from these year-round measurements agreed with the reported results of 6.5 to 4.6
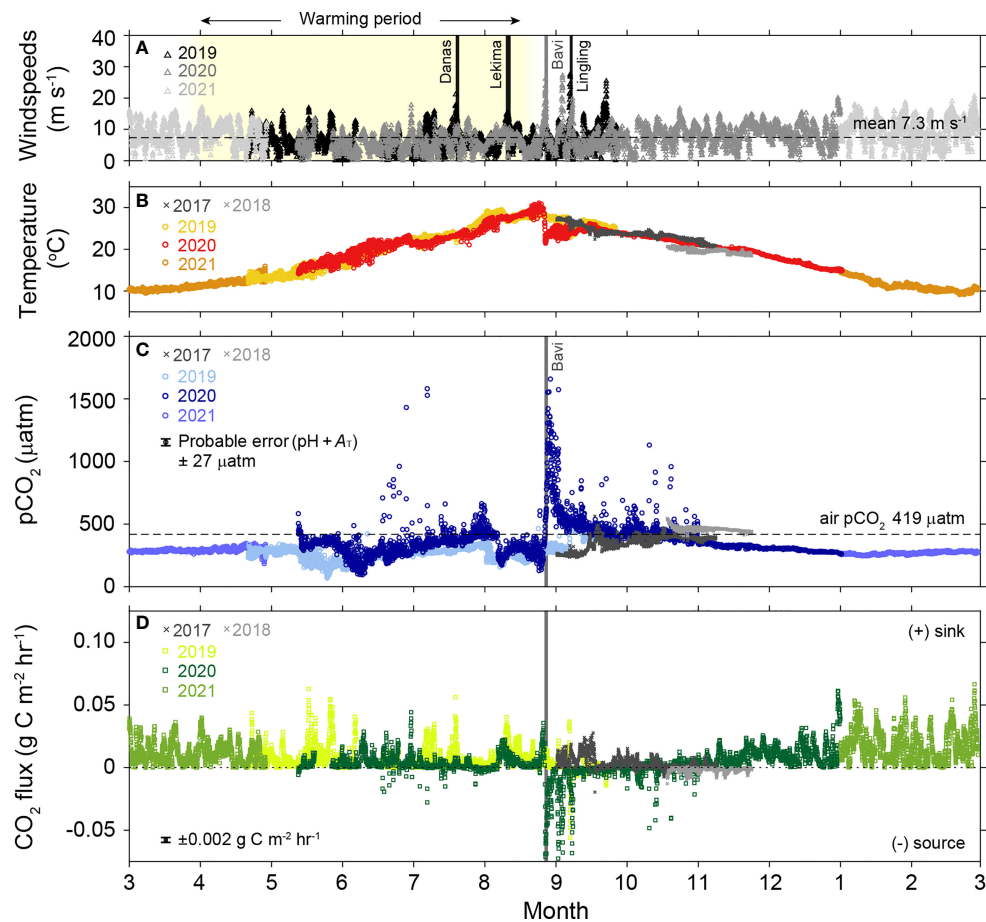
FIGURE 4 | Changes in **(A)** windspeeds, **(B)** sea surface temperature, **(C)** seawater pCO_2, and **(D)** air–sea CO_2 flux for the period 2017–2021. Shaded area in **(A)** indicates the warming period from April to mid-August. Vertical lines in black represent the landing periods of major typhoons. The solid horizontal line in **(C)** indicates the level of mean pCO_2 of the air. The probable error in pCO_2 is the square root of the sum of the squared errors associated with measurements of pH and A_T. The error in the CO_2 flux was propagated from the pCO_2 error.

mmol C m^{-2} d^{-1} (4.9 to 3.4 mmol C m^{-2} d^{-1} using the same k used in this study) associated with the river plume and the outer estuary, respectively (Guo et al., 2015). However, we found large differences in the net air–sea CO_2 fluxes for spring and winter: the net air–sea CO_2 fluxes for spring (20.3 mmol C m^{-2} d^{-1}) and winter (31.5 mmol C m^{-2} d^{-1}) were 2–4 times higher than the previous estimates (Tseng et al., 2011; Guo et al., 2015).

Mechanisms Responsible for C Uptake by the ECS

Both high plankton biomass in spring and summer and a large temperature drop from summer to winter, collectively, contributed to the substantial C sink by the northern ECS; their effects on the net air–sea CO_2 flux were decoupled in terms of season. An increase in planktonic biomass during the growing season spread vertically into the shallow shelf water (< 70 m depth) and the resultant organic matter was either buried into the shallow sediments or moved laterally. These

biological activities lowered the water-column pCO_2 levels, which were lower than the atmospheric pCO_2 levels throughout the warming months (April–August), except for a short transition time to the cooling period, during which the surface pCO_2 reached levels similar to or slightly greater than the atmospheric levels. In particular, a rapid increase in planktonic biomass during the warming period counteracted nearly all the temperature-driven pCO_2 increase (~ 85%, **Figure 6A**). As the season developed into a full winter condition, the water column was substantially cooled by as much as 17°C (August–March, **Figure 4B**) and this temperature drop lowered the water column pCO_2 values by as much as 175 µatm at Ieodo. The observed reduction of the surface pCO_2 during the cooling months was surprisingly consistent with the thermodynamic expectations (> 75%, **Figure 6B**). In particular, during the winter, both the low pCO_2 levels and high air–sea CO_2 exchange rates, driven by a large temperature drop and high windspeeds, respectively, acted in concert to increase the C uptake by the northern ECS and made the basin an even stronger C sink.
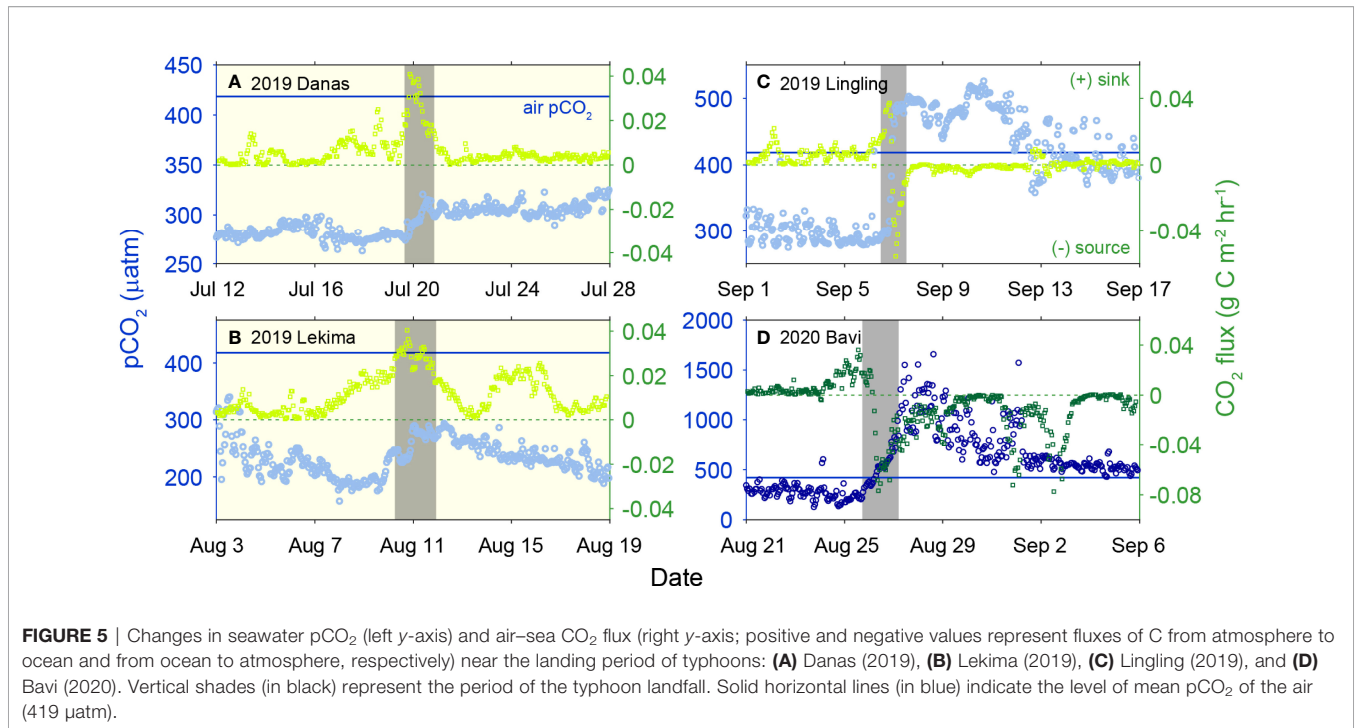
FIGURE 5 | Changes in seawater pCO_2 (left y-axis) and air–sea CO_2 flux (right y-axis; positive and negative values represent fluxes of C from atmosphere to ocean and from ocean to atmosphere, respectively) near the landing period of typhoons: **(A)** Danas (2019), **(B)** Lekima (2019), **(C)** Lingling (2019), and **(D)** Bavi (2020). Vertical shades (in black) represent the period of the typhoon landfall. Solid horizontal lines (in blue) indicate the level of mean pCO_2 of the air (419 μatm).

Reported water properties of the northern ECS appeared to be an additional favorable factor for the northern ECS to be a perennial C sink—the continental shelf pump (Tsunogai et al., 1999). Isopycnal mixing (*via* diffusive and advective flows) in the ECS tends to transport the shelf waters to the deeper layers of the Kuroshio region, which transports dissolved inorganic C

FIGURE 6 | Estimated temperature-driven changes in seawater pCO_2 (4% pCO_2 increase °C^{-1}) and those measured at *in situ* condition during **(A)** the warming months (mid-July values minus April values; excluding the landing period of typhoons) versus **(B)** the cooling months (March values minus November values) for the period 2017–2021. The differences between temperature-driven changes in pCO_2 and *in situ* values indicate the changes caused by nonthermal factors, mostly biology.

to the open ocean. A large temperature drop from summer to winter in the shallow continental shelf zone, including our study area, resulted in greater CO_2 flux into the ocean (resulting from high CO_2 solubility at low temperatures) and the rapid formation of dense water (resulting from rapid heat loss while cooling). Both of these factors enable the effective transport of C from the shallow northern ECS to the open ocean. The C export from the northern ECS to the open ocean was also reported by Chen and Wang (1999) to be in the form of both particulate and dissolved organic C. The organic C produced by phytoplankton on the ECS shelf was exported as DOC (8%) to the offshore water column or exported as POC (10%) to the shelf and offshore sedimentary environments to the shelf and offshore sedimentary environments. The downslope transport of POC accounted for ~40% of the inorganic C transport to offshore. The transport of the shelf water to the open ocean *via* isopycnal flow greatly facilitated the transport of both inorganic and organic C to the open ocean, which contributed to substantial uptake of atmospheric CO_2 by the northern ECS shelf region.
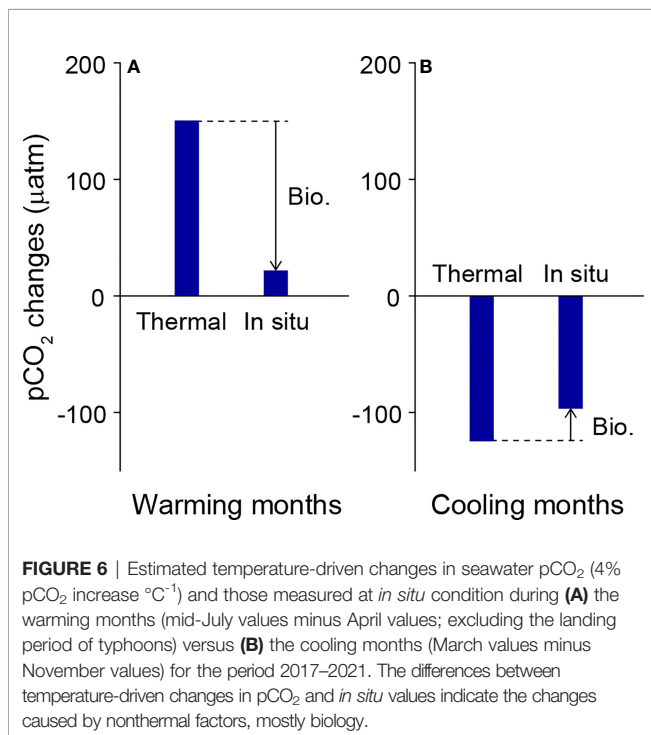
Future Projections of C Uptake by the ECS

How the C uptake status of the northern ECS has evolved and how it will change are noteworthy. Because the northern ECS has increasingly received anthropogenic nutrients over the past 40 years *via* the CDW and, to a lesser extent, atmospheric deposition (Kim et al., 2020; Zheng and Zhai, 2021), the region has grown fertile in phytoplankton and thus, removed surface C in the form of organic matter. Much of the organic matter has likely been buried in the shallow marine sediments there. Increasing organic C production and the corresponding burial

of organic C in shallow sediments have probably strengthened the northern ECS as a C sink over the past 40 years, particularly in summer (Chou et al., 2013). Moreover, the nutrient-reinforced C-rich bottom water may have affected the interannual variations in the winter C uptake status (Chou et al., 2011). However, the C sink of the northern ECS will not increase indefinitely in proportion to the increasing input of nutrients from the Changjiang River but is likely to increase until nitrate (N) acts as a limiting nutrient for organic C production (i.e., until N increases to the levels estimated on the basis of phosphate (P) concentrations multiplied by 16) (Moon et al., 2021). Further increase in seawater N concentration exceeding an N:P ratio of 16 will no longer enhance the biological production in the northern ECS. Instead, excess N (= [N] – 16 × [P]) spreads into adjacent regions that are still N deficient and progressively makes them fertile. Eventually, it could expand the C sink area in the ECS. The increasing input of nutrients will make the entire ECS a stronger C sink. Conversely, a scenario of the C sink weakening by the northern ECS is equally feasible because of a reduction of nutrient supply to this area by controlling the Changjiang river discharge *via* the operation of the Three Gorges Dam (Tseng et al., 2011).

Another factor that has yet to be fully explored is the effect of typhoons on the net air–sea CO_2 flux in the entire ECS. Year-round data collected from a mooring at the central ECS located outside the influence of the CDW showed that a large CO_2 efflux induced by typhoons dictated the overall C status of the central and southern ECS by switching the basin from a weak C sink to a weak C source (Wu et al., 2021). Unlike the typhoons in the central and southern ECS, those in the northern ECS exerted contrasting effects on the net air–sea CO_2 flux, depending on the levels of seawater pCO_2 at the time of typhoon passage (**Figure 5**). When the typhoon passage occurs during the warming period, low pCO_2 levels (resulting from phytoplankton growth) and a high rate of CO_2 exchange (because of high windspeeds) would greatly enhance CO_2 uptake. By contrast, during the cooling period, higher oceanic pCO_2 levels (because of the addition of CO_2-rich bottom water to the surface by the increased vertical mixing) would result in considerable CO_2 effluxes. Over the two years (2019–2020), two competing effects of typhoon passage on the net air–sea CO_2 fluxes approximately canceled out each other because typhoons meeting the two different cases were equal in number during the observational period. However, the entire ECS will likely be struck by typhoons more frequently in the future as the sea surface temperature in the region increases at an unprecedented rate. With the increasing frequency of typhoon passage, the future status of the ECS as a C sink or a C source will depend on the timing of typhoon passage.

CONCLUSION

Using discrete surface C measurements between Ieodo and Jeju Island (2015–2021) and *in situ* continuous measurements at Ieodo (seasonal coverage for 2017–2019 and the year-round coverage for 2020–2021), we concluded that the northern ECS was a substantial sink of atmospheric CO_2 during most seasons (December to August). Such large C uptake by the northern ECS shifted the entire ECS toward a moderate C sink on an annual basis. The competing effects (reinforcing the C-sink vs. inducing the C-source) of episodic typhoon passage depending on the bottom water C accumulation by the timing of typhoon passages transiently deviated the CO_2 system. Nonetheless, the northern ECS is likely to remain as a large C sink unless the current input of anthropogenic nutrients to the northern ECS shows a sudden change. The present study provides observational and mechanistic lines of evidence for confirming the continental shelf C pump (Tsunogai et al., 1999).

AUTHOR CONTRIBUTIONS

KL formulated the research question. KL, J-MK and G-SL analyzed the data, and J-MK and KL wrote the paper together. G-SL, EL, J-YJ, JL and I-SH contributed to C measurements for this paper. All authors contributed to the article and approved the submitted version.

ACKNOWLEDGMENTS

SUPPLEMENTARY MATERIAL

The Supplementary Material for this article can be found online at: https://www.frontiersin.org/articles/10.3389/fmars.2022.919249/full#supplementary-material

REFERENCES

Cai, W.-J., Wang, Y., and Hodson, R. (1998). Acid-Base Properties of Dissolved Organic Matter in the Estuarine Waters of Georgia, USA. *Geochim. Cosmochim. Acta* 62, 473–483. doi: 10.1016/S0016-7037(97)00363-3

Cao, Z., Yang, W., Zhao, Y., Guo, X., Yin, Z., Du, C., et al. (2019). Diagnosis of CO_2 Dynamics and Fluxes in Global Coastal Oceans. *Natl. Sci. Rev.* 7 (4), 786–797. doi: 10.1093/nsr/nwz105

Chang, C.-P. (2004). *East Asian Monsoon* (Singapore: World Scientific).

Chen, C.-T. A., and Wang, S.-L. (1999). Carbon, Alkalinity and Nutrient Budgets on the East China Sea Continental Shelf. *J. Geophys. Res.* 104 (C9), 20675–20686. doi: 10.1029/1999JC900055

Choi, S.-D., Lee, K., and Chang, Y.-S. (2002). Large Rate of Uptake of Atmospheric Carbon Dioxide by Planted Forest Biomass in Korea. *Global Biogeochem. Cycle.* 16 (4), 1089. doi: 10.1029/2002GB001914

Chou, W. C., Gong, G. C., Cai, W. J., and Tseng, C. M. (2013). Seasonality of CO_2 in Coastal Oceans Altered by Increasing Anthropogenic Nutrient Delivery From Large Rivers: Evidence From the Changjiang–East China Sea System. *Biogeosciences* 10 (6), 3889–3899. doi: 10.5194/bg-10-3889-2013

Chou, W.-C., Gong, G.-C., Tseng, C.-M., Sheu, D. D., Hung, C.-C., Chang, L.-P., et al. (2011). The Carbonate System in the East China Sea in Winter. *Mar. Chem.* 123 (1), 44–55. doi: 10.1016/j.marchem.2010.09.004

Clayton, T. D., and Byrne, R. H. (1993). Spectrophotometric Seawater pH Measurements: Total Hydrogen Ion Concentration Scale Calibration of M-Cresol Purple and at-Sea Results. *Deep. Sea. Res. Part I.: Oceanog. Res. Pap.* 40 (10), 2115–2129. doi: 10.1016/0967-0637(93)90048-8

Dai, M., Cao, Z., Guo, X., Zhai, W., Liu, Z., Yin, Z., et al. (2013). Why Are Some Marginal Seas Sources of Atmospheric CO_2? *Geophys. Res. Lett.* 40 (10), 2154–2158. doi: 10.1002/grl.50390

Deng, X., Zhang, G.-L., Xin, M., Liu, C.-Y., and Cai, W.-J. (2021). Carbonate Chemistry Variability in the Southern Yellow Sea and East China Sea During Spring of 2017 and Summer of 2018. *Sci. Tot. Environ.* 779, 146376. doi: 10.1016/j.scitotenv.2021.146376

Fong, M. B., and Dickson, A. G. (2019). Insights From GO-SHIP Hydrography Data Into the Thermodynamic Consistency of CO_2 System Measurements in Seawater. *Mar. Chem.* 211, 52–63. doi: 10.1016/j.marchem.2019.03.006

Guo, X. H., Zhai, W. D., Dai, M. H., Zhang, C., Bai, Y., Xu, Y., et al. (2015). Air–Sea CO_2 Fluxes in the East China Sea Based on Multiple-Year Underway Observations. *Biogeosciences* 12 (18), 5495–5514. doi: 10.5194/bg-12-5495-2015

Kim, D., Choi, S.-H., Shim, J., Kim, K. H., and Kim, C.-H. (2013). Revisiting the Seasonal Variations of Sea-Air CO_2 Fluxes in the Northern East China Sea. *Terres. Atmosph. Ocean. Sci.* 24, 409. doi: 10.3319/TAO.2012.12.06.01(Oc

Kim, H.-C., and Lee, K. (2009). Significant Contribution of Dissolved Organic Matter to Seawater Alkalinity. *Geophys. Res. Lett.* 36 (20), L20603. doi: 10.1029/2009gl040271

Kim, J.-M., Lee, K., Han, I.-S., Lee, J.-S., Choi, Y.-H., Lee, J. H., et al. (2020). Anthropogenic Nitrogen-Induced Changes in Seasonal Carbonate Dynamics in a Productive Coastal Environment. *Geophys. Res. Lett.* 47 (17), e2020GL088232. doi: 10.1029/2020GL088232

Ko, Y. H., Lee, K., Noh, J. H., Lee, C. M., Kleypas, J. A., Jeong, H. J., et al. (2016). Influence of Ambient Water Intrusion on Coral Reef Acidification in the Chuuk Lagoon, Located in the Coral-Rich Western Pacific Ocean. *Geophys. Res. Lett.* 43 (8), 3830–3838. doi: 10.1002/2016gl068234

Lee, K., Chris, S., Tanhua, T., Kim, T.-W., Feely, R., and Kim, H.-C. (2011). Roles of Marginal Seas in Absorbing and Storing Fossil Fuel CO_2. *Energy Environ. Sci.* 4, 1133–1146. doi: 10.1039/C0EE00663G

Lee, K., Kim, T.-W., Byrne, R. H., Millero, F. J., Feely, R. A., and Liu, Y.-M. (2010). The Universal Ratio of Boron to Chlorinity for the North Pacific and North Atlantic Oceans. *Geochim. Cosmochim. Acta* 74 (6), 1801–1811. doi: 10.1016/j.gca.2009.12.027

Lee, C.-H., Lee, K., Ko, Y. H., and Lee, J.-S. (2021). Contribution of Marine Phytoplankton and Bacteria to Alkalinity: An Uncharacterized Component. *Geophys. Res. Lett.* 48 (19), e2021GL093738. doi: 10.1029/2021GL093738

Lee, K., Lee, C.-H., Lee, J.-H., Han, I.-S., and Kim, M. (2019). Deviation of Boron Concentration From Predictions Using Salinity in Coastal Environments. *Geophys. Res. Lett.* 46 (9), 4809–4815. doi: 10.1029/2019gl082520

Lee, K., Millero, F. J., Byrne, R. H., Feely, R. A., and Wanninkhof, R. (2000). The Recommended Dissociation Constants for Carbonic Acid in Seawater. *Geophys. Res. Lett.* 27 (2), 229–232. doi: 10.1029/1999gl002345

Lee, K., Millero, F. J., and Campbell, D. M. (1996). The Reliability of the Thermodynamic Constants for the Dissociation of Carbonic Acid in Seawater. *Mar. Chem.* 55 (3), 233–245. doi: 10.1016/S0304-4203(96)00064-3

Lee, K., Tong, L. T., Millero, F. J., Sabine, C. L., Dickson, A. G., Goyet, C., et al. (2006). Global Relationships of Total Alkalinity With Salinity and Temperature in Surface Waters of the World's Oceans. *Geophys. Res. Lett.* 33 (19):L19605. doi: 10.1029/2006GL027207

Li, D., Ni, X., Wang, K., Zeng, D., Wang, B., Jin, H., et al. (2021). Biological CO_2 Uptake and Upwelling Regulate the Air-Sea CO_2 Flux in the Changjiang Plume Under South Winds in Summer. *Front. Mar. Sci.* 8 (1207). doi: 10.3389/fmars.2021.709783

Lueker, T. J., Dickson, A. G., and Keeling, C. D. (2000). Ocean Pco_2 Calculated From Dissolved Inorganic Carbon, Alkalinity, and Equations for K_1 and K_2: Validation Based on Laboratory Measurements of CO_2 in Gas and Seawater at Equilibrium. *Mar. Chem.* 70 (1), 105–119. doi: 10.1016/S0304-4203(00)00022-0

McElligott, S., Byrne, R. H., Lee, K., Wanninkhof, R., Millero, F. J., and Feely, R. A. (1998). Discrete Water Column Measurements of CO_2 Fugacity and pH_T in Seawater: A Comparison of Direct Measurements and Thermodynamic Calculations. *Mar. Chem.* 60 (1), 63–73. doi: 10.1016/S0304-4203(97)00080-7

Mehrbach, C., Culberson, C. H., Hawley, J. E., and Pytkowicx, R. M. (1973). Measurement of the Apparent Dissociation Constants of Carbonic Acid in Seawater at Atmospheric Pressure. *Limnol. Oceanog.* 18 (6), 897–907. doi: 10.4319/lo.1973.18.6.0897

Millero, F. J. (1995). Thermodynamics of the Carbon Dioxide System in the Oceans. *Geochim. Cosmochim. Acta* 59 (4), 661–677. doi: 10.1016/0016-7037(94)00354-O

Millero, F. J., Graham, T. B., Huang, F., Bustos-Serrano, H., and Pierrot, D. (2006). Dissociation Constants of Carbonic Acid in Seawater as a Function of Salinity and Temperature. *Mar. Chem.* 100 (1), 80–94. doi: 10.1016/j.marchem.2005.12.001

Moon, J.-Y., Lee, K., Lim, W.-A., Lee, E., Dai, M., Choi, Y.-H., et al. (2021). Anthropogenic Nitrogen Is Changing the East China and Yellow Seas From Being N Deficient to Being P Deficient. *Limnol. Oceanog.* 66 (3), 914–924. doi: 10.1002/lno.11651

Najjar, R. G., Herrmann, M., Alexander, R., Boyer, E. W., Burdige, D. J., Butman, D., et al. (2018). Carbon Budget of Tidal Wetlands, Estuaries, and Shelf Waters of Eastern North America. *Global Biogeochem. Cycle.* 32 (3), 389–416. doi: 10.1002/2017GB005790

Park, G.-H., Lee, K., Tishchenko, P., Min, D.-H., Warner, M. J., Talley, L. D., et al. (2006). Large Accumulation of Anthropogenic CO_2 in the East (Japan) Sea and its Significant Impact on Carbonate Chemistry. *Global Biogeochem. Cycle.* 20 (4):GB4013. doi: 10.1029/2005GB002676

Piao, S., Fang, J., Ciais, P., Peylin, P., Huang, Y., Sitch, S., et al. (2009). The Carbon Balance of Terrestrial Ecosystems in China. *Nature* 458 (7241), 1009–1013. doi: 10.1038/nature07944

Shim, J., Kim, D., Kang, Y. C., Lee, J. H., Jang, S.-T., and Kim, C.-H. (2007). Seasonal Variations in Pco_2 and Its Controlling Factors in Surface Seawater of

the Northern East China Sea. *Continent. Shelf. Res.* 27 (20), 2623–2636. doi: 10.1016/j.csr.2007.07.005

Thomas, H., Schiettecatte, L.-S., Suykens, K., Koné, M., Shadwick, E., Prowe, A. E. F., et al. (2009). Enhanced Ocean Storage From Anaerobic Alkalinity Generation in Coastal Sediments. *Biogeosciences* 6, 267–274. doi: 10.5194/bg-6-267-2009

Tseng, C.-M., Liu, K.-K., Gong, G.-C., Shen, P.-Y., and Cai, W.-J. (2011). CO_2 Uptake in the East China Sea Relying on Changjiang Runoff Is Prone to Change. *Geophys. Res. Lett.* 38 (24), L24609. doi: 10.1029/2011GL049774

Tsunogai, S., Watanabe, S., and Sato, T. (1999). Is There a "Continental Shelf Pump" for the Absorption of Atmospheric CO_2? *Tellus. B.* 51 (3), 701–712. doi: 10.3402/tellusb.v51i3.16468

Wang, S.-L., Arthur Chen, C.-T., Hong, G.-H., and Chung, C.-S. (2000). Carbon Dioxide and Related Parameters in the East China Sea. *Continent. Shelf. Res.* 20 (4), 525–544. doi: 10.1016/S0278-4343(99)00084-9

Wanninkhof, R. (2014). Relationship Between Wind Speed and Gas Exchange Over the Ocean Revisited. *Limnol. Oceanog.: Methods* 12 (6), 351–362. doi: 10.4319/lom.2014.12.351

Wu, Y., Dai, M., Guo, X., Chen, J., Xu, Y., Xu, D., et al. (2021). High-Frequency Time-Series Autonomous Observations of Sea Surface Pco_2 and pH. *Limnol. Oceanog.* 66, 588–606. doi: 10.1002/lno.11625

Zhai, W., and Dai, M. (2009). On the Seasonal Variation of Air–Sea CO_2 Fluxes in the Outer Changjiang (Yangtze River) Estuary, East China Sea. *Mar. Chem.* 117 (1), 2–10. doi: 10.1016/j.marchem.2009.02.008

Zhang, J., Guo, X., and Zhao, L. (2021). Budget of Riverine Nitrogen Over the East China Sea Shelf. *Environ. Pollut.* 289, 117915. doi: 10.1016/j.envpol.2021.117915

Zheng, L.-w., and Zhai, W.-d. (2021). Excess Nitrogen in the Bohai and Yellow Seas, China: Distribution, Trends, and Source Apportionment. *Sci. Tot. Environ.* 794, 148702. doi: 10.1016/j.scitotenv.2021.148702